Tight-binding study of the optical properties of GaN/AlN polar and nonpolar quantum wells

A. Molina *, A. García-Cristóbal and A. Cantarero

Materials Science Institute, University of Valencia, P.O. Box 22085, 46071 Valencia, Spain

Abstract

The electronic structure of wurtzite semiconductor superlattices (SLs) and quantum wells (QWs) is calculated by using the empirical tight-binding method. The basis used consists of four orbitals per atom (sp^3 model), and the calculations include the spin-orbit coupling as well as the strain and electric polarization effects. We focus our study on GaN/AlN quantum wells grown both in polar (C) and nonpolar (A) directions. The band structure, wave functions and optical absorption spectrum are obtained and compared for both cases.

Key words: Tight-binding, Semiconductors III-V, Quantum well, Nitrides,
PACS: 71.15 Ap, 71.20 Nr, 73.21 Fg, 77.84.Bw

1 Introduction

The wide bandgap group III-nitride compounds AlN and GaN have attracted a great interest due to their potential applications in short-wave light emitting devices [1]. Usually, these materials are grown with the wurtzite crystalline structure [2]. Due to their different lattice parameters, the heterostructures composed by them are strained, with the corresponding effect in their electronic structure [3]. Another very important feature of GaN/AlN heterostructures is the appearance of internal electric fields due to the presence of different electrical polarization in both semiconductors. This polarization has two contributions, spontaneous and piezoelectric. The spontaneous polarization,

* Corresponding author. Tel +34 963543260.
Email address: alejandro.molina@uv.es (A. Molina).

which is intrinsic to the material, has its origin in the non-centrosymmetric nature of the wurtzite crystal and it points along the C-axis ([0001] direction) [4]. The piezoelectric polarization arises as a consequence of the strained state of the structure and, in the absence of shearing deformation, also points along the C-axis. Therefore, the GaN/AlN superlattices (SLs) and quantum wells (QWs) grown along the C-axis exhibit huge built-in electric fields which affect their electronic and optical properties [2]. These fields, which can be useful in some sensor applications [5], are often detrimental for optoelectronic devices. One possible way out of this problem is the growth of superlattices along nonpolar directions perpendicular to the C-axis, such as the the $[1\bar{1}00]$ (M-axis) or $[11\bar{2}0]$ (A-axis) [6]. On the other hand, the nonpolar heterostructures are expected to exhibit a noticeable in-plane anisotropy as compared to the polar ones grown along the C-axis [7].

In order to study the differences between the optical properties of polar and nonpolar GaN/AlN QWs, we present in this work numerical calculations of the band structure, confined states and optical absorption of quantum wells grown along C and A directions (C-QWs and A-QWs henceforth).

2 Theoretical Model

The calculation of the electronic structure is performed within the framework of the empirical tight-binding method, as applied to the wurtzite hexagonal symmetry [8] and including the spin-orbit coupling [9]. The model uses a basis of four orbitals per atom (sp^3 model) and the interaction between atoms is restricted to nearest-neighbors. The tight-binding parameters are taken from [10].

The superlattice geometry is generated by defining a supercell $(\mathrm{AlN})_m(\mathrm{GaN})_n$, where m and n indicate the number of layers (each layer contains four atoms) in each material, to which periodic boundary conditions are imposed. Therefore, the quantum well is modeled in this work as a superlattice with thick-enough barrier to avoid coupling between adjacent wells. Besides, the superlattice potential is introduced by offseting the diagonal elements in the tight-binding Hamiltonian matrices of both materials by the reported value of the valence band offset, VBO=0.80 eV [2]. The modification of the interatomic distances resulting from the lattice mismatch is calculated by using the valence force field method [11], and introduced in the tight-binding model by means of Harrison's rules [12]. It is to be noticed that the values of the strain obtained with this atomistic model agree well with those given by continuum elasticity theory. In the case of C-QWs, the strain results are also used to calculate the piezoelectric polarization in each material, which together with the intrinsic spontaneous polarizations [13], lead to the appearance of an elec-

trostatic potential [14]. This potential is in turn added to the diagonal of the Hamiltonian matrix. When dealing with A-QWs the polarization does not exhibit discontinuities at the interfaces and therefore they are free of electrostatic field. Once the Hamiltonian matrix is constructed, the band structure and wave functions are obtained by standard diagonalization techniques, and the optical absorption spectra are computed following the procedure explained in [15], where the individual transitions are broadened with a Lorentzian of width 10 meV.

3 Numerical Results

In this Section we present some selected numerical results in order illustrate the main differences in the optical properties of C- and A-QWs.

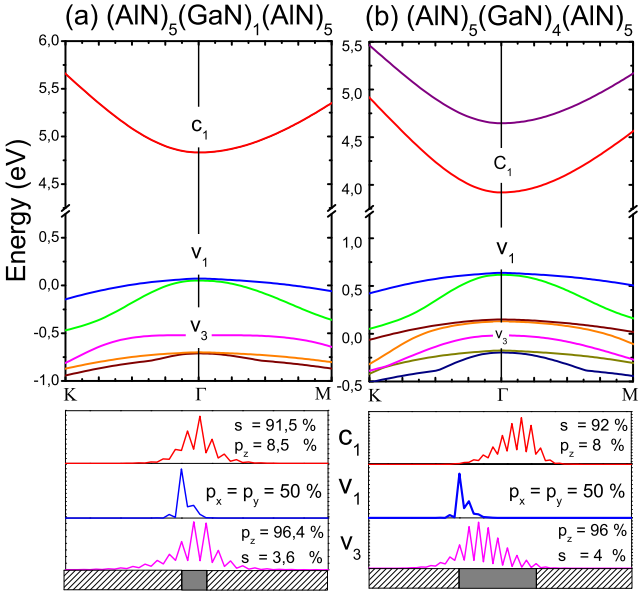

Figure 1. Band structure of two QWs of different thickness: (a) $(AlN)_5(GaN)_1(AlN)_5$ (0.5 nm) and (b) $(AlN)_5(GaN)_4(AlN)_5$ (2.0 nm). The bottom pictures show the probability density of the lowest confined states in the point Γ, with indications of the mixture of atomic symmetry. The notation of Kobayashi [8] is used for the Brillouin zone points.

First, we investigate the electronic structure of C-QWs. The band structure of $(AlN)_5(GaN)_1(AlN)_5$ and $(AlN)_5(GaN)_4(AlN)_5$ C-QWs is presented in Fig. 1. The equivalent well widths are 0.5 nm and 2.0 nm, respectively. It is noticeable a large reduction in the fundamental energy gap, from 4.76 eV to 3.28 eV, with increasing QW thickness. This reduction is caused mainly by the tilt of the band edges induced by the built-in electric field (quantum-confined Stark

effect, QCSE). The QCSE also affects the distribution of the confined electron and hole wavefunctions, which acquire a notable separation for the wider QW, as illustrated by the probability density shown in the bottom pictures of Fig. 1. Another important result concerns the symmetry of the wave functions, which is characterized in Fig. 1 by the percent contribution of the atomic orbital symmetry to the integrated probability density.

Figure 2 shows the calculated optical absorption spectra of the same two C-QWs studied in Fig. 1. The spectra denoted as $\boldsymbol{\sigma} \perp$C correspond to the situations in which the light polarization vector $\boldsymbol{\sigma}$ lies in the plane of the well, as it would happen in a normal incidence absorption experiment. Since the absorption spectrum is essentially the same for any $\boldsymbol{\sigma}$ contained in the well plane, we represent in Fig. 2 an average over two orthogonal directions. The spectra denoted as $\boldsymbol{\sigma} \parallel$C would be relevant for the analysis of optical absorption with light incidence from the lateral side of the structure. As shown in Fig. 2, the redshift of the absorption edge due to the v_1-c_1 transition with increasing well width is accompanied by a huge reduction in the value of the optical absorption coefficient. This is explained by the electron-hole separation displayed in Fig. 1 which dramatically reduces the oscillator strength. On the other hand, the differences in the spectra depending on the light polarization are also noticeable. The edge of the $\boldsymbol{\sigma} \parallel$C spectra are displaced to higher energies as compared to their $\boldsymbol{\sigma} \parallel$C counterparts. This is because in the former case the light can only couple states with dominant s and p_z atomic contributions, and this situation arises only for the higher-energy transition v_3-c_1.

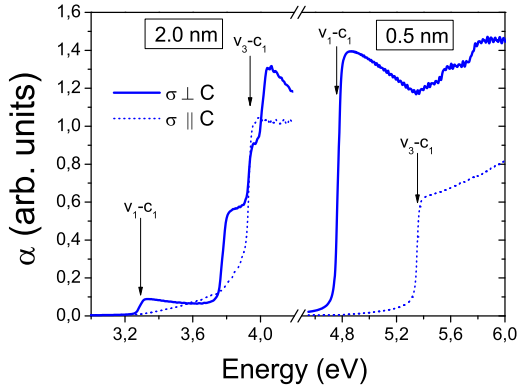

Figure 2. Optical absorption spectra of two C-QWs, $(AlN)_5(GaN)_1(AlN)_5$ (well width equal to 0.5 nm) and $(AlN)_5(GaN)_4(AlN)_5$ (2.0 nm), for different orientations of the light polarization vector (see text). The transitions between the Γ-states of Fig. 1 are marked with arrows.

The results obtained for a nonpolar $(AlN)_5(GaN)_1(AlN)_5$ A-QW are summarized in Fig. 3. The inset of the figure shows the in-plane band dispersion,

which now exhibits a strong anisotropy between the two orthogonal directions $\Gamma \rightarrow A$ ($\boldsymbol{k} \parallel [0001]$)) and $\Gamma \rightarrow M$ ($\boldsymbol{k} \parallel [1\bar{1}00]$)). Accordingly, the optical absorption spectra polarized along the two in-plane perpendicular directions, $\boldsymbol{\sigma}$ ∥C and $\boldsymbol{\sigma}$ ∥M, are now rather different. Their absorption edge occurs at slightly different energies, since they correspond to different transitions, marked as 1 and 2 in the band structure diagram of the inset. The intensities of these transitions are different. This in-plane anisotropy is typical of nonpolar heterostructures [7]. The optical spectrum for polarization along the growth direction, $\boldsymbol{\sigma}$ ∥A, ressembles that of $\boldsymbol{\sigma}$ ∥C, but with a smaller intensity. The detailed explanation of these differences can be traced back to the mixed symmetry character of the valence band states as obtained from the contribution of the atomic orbitals.

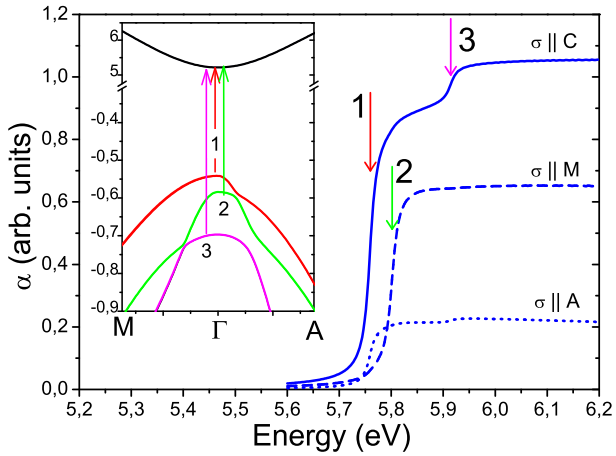

Figure 3. Optical absorption spectra of the A-QW defined by the sequence of layers $(AlN)_5(GaN)_1(AlN)_5$ (well width equal to 0.3 nm), for different orientations of the light polarization vector (see text). The inset shows the band structure of the QW, and the transitions between the Γ-states are marked with arrows in the spectra.

As we mentioned in the Introduction, when a QW is grown in A-plane, it is free of internal field [6], and therefore does not show the QCSE. In order to illustrate this fact, Fig. 4 presents a comparison of the optical absorption for C- and A-QW of the same width, ∼ 2 nm. If there were no electric field in the C-QW, the fundamental gap of the two QWs should be roughly the same. In the actual case shown Fig. 4, the QCSE results in a redshift of ∼700 meV of the C-QW spectrum with respect to that of the A-QW, and a reduction of the absorption intensity by a factor of ∼ 10.

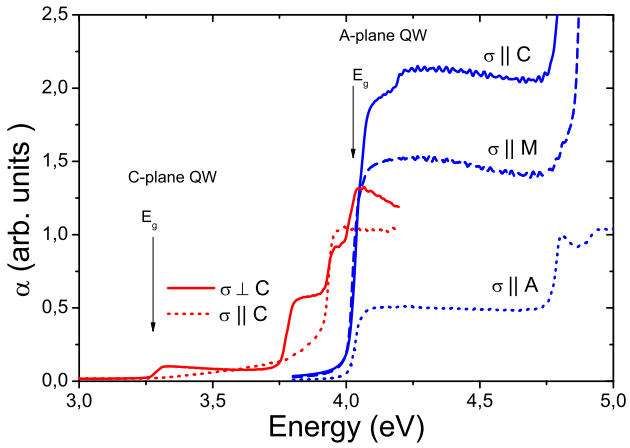

Figure 4. Optical absorption spectra of C- and A-QW of the same width, ~ 2 nm. The same notation for the light polarization as in Figs. 2 and 3 is followed. The arrows mark the fundamental energy gap.

4 Conclusions

In summary, we have computed the electronic structure and optical absorption of polar (C) and nonpolar (A) wurtzite QWs by using an atomistic tight-binding approach. The numerical results illustrate the influence of the QCSE in C-QWs and its dependence on the well width. The comparison with the corresponding results of A-QWs clearly shows the expected differences in the optical properties, namely no redshift and increased intensity for the nonpolar QWs. Moreover, the optical absorption has been calculated for different orientation of the light polarization vector, and a strong in-plane anisotropy has been found for the case of A-QWs.

5 Acknowledgements

This work has been supported by the European Network of Excellence SANDIE.

References

[1] S. Nakamura, S. Pearton, G. Fasol, The Blue Laser Diode, Springer, Berlin, 2000.

[2] B. Monemar, G. Pozina, Progress in Quantum Electronics, 24 (2000) 239-290.

[3] S. L. Chuang, C. S. Chang, Phys. Rev. B 54 (1996), 2491-2504.
[4] F. Bernardini and V. Fiorentini. Appl. Surf. Sci. 166 (2000) 23-29.
[5] O. Ambacher, J. Phys. D: Appl. Phys. 31 (1998), 2653-2710
[6] T. Paskova (ed), Nitrides with Nonpolar Surfaces: Growth, Properties, and Devices, Wiley, 2008.
[7] P. Misra , U. Behn, O. Brandt, H. T. Grahn, B. Imer, S. Nakamura, S. P. DenBaars, J. S. Speck, Applied Physics Letters 88 (2006), 161920.
[8] A. Kobayashi, O.F. Sankey, S.M. Volz, D. Dow, Phys. Rev. B 28 (1983) 935.
[9] D.J. Chadi, Phys. Rev. B 16 (1977) 790.
[10] D.W. Jenkins, J.D. Dow, Phys. Rev. B 39 (1989) 3317.
[11] P.N. Keating, Phys. Rev. 145 (1966) 637.
[12] W.A. Harrison, Electronic Structure of Solids, Dover, New York, 1973.
[13] I. Vurgaftman, J.R. Meyer. J. Appl. Phys 94 (2003) 3675.
[14] B.K. Ridley, W.J. Schaff, L.F. Eastman, J. Appl. Phys 94 (2003) 3972.
[15] A. Di Carlo. Phys. Stat. Sol. (b) 217 (2000) 703.